



**Correlating conduction properties with the molecular symmetry: segregation of Z and E isomers in the charge-assisted, halogen-bonded cocrystal [(Z,E)-Me<sub>2</sub>I<sub>2</sub>TTF]<sub>2</sub>Br**

Journal:	<i>ChemComm</i>
Manuscript ID	CC-COM-09-2015-008176.R1
Article Type:	Communication
Date Submitted by the Author:	19-Oct-2015
Complete List of Authors:	Jeannin, olivier; UMR 6226 CNRS, MaCSE Canadell, Enrique; Campus de la UAB, Institut de Ciencia de Materials de Barcelona Auban-Senzier, Pascale; Université Paris-Sud, Lab. Physique des Solides Fourmigue, Marc; CNRS, Sciences Chimiques de Rennes

## Correlating conduction properties with the molecular symmetry: segregation of *Z* and *E* isomers in the charge-assisted, halogen-bonded cocrystal [(*Z,E*)-Me<sub>2</sub>I<sub>2</sub>TTF]<sub>2</sub>Br<sup>†</sup>

Received 00th January 20xx,  
Accepted 00th January 20xx

DOI: 10.1039/x0xx00000x

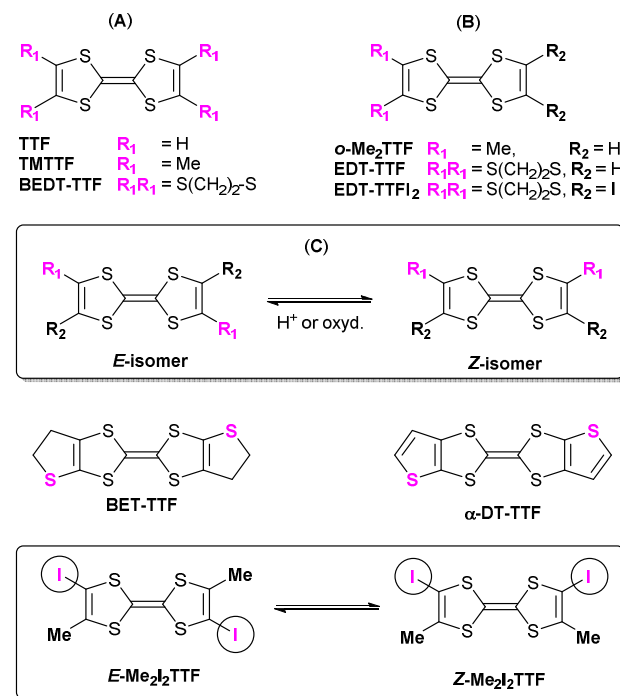
www.rsc.org/

Olivier Jeannin,<sup>a</sup> Enric Canadell,<sup>b</sup> Pascale Auban-Senzier<sup>c</sup> and Marc Fourmigué<sup>\*a</sup>

**The *Z* and *E* isomers of the iodinated TTF derivative (*Z,E*)-Me<sub>2</sub>I<sub>2</sub>-TTF co-crystallize in its mixed-valence salt with the Br<sup>-</sup> anion, into segregated *Z* and *E* stacks, each of them with a different charge localization pattern, also revealed by charge-assisted halogen bonding.**

Molecular conductors<sup>1</sup> offer a fertile playground where chemistry and physics meet in the search for materials with new and exotic electronic properties. Such systems exhibit strong electronic correlations<sup>2</sup> and offer a real promise in such direction. At the forefront of this effort, structural chemistry and crystal engineering play a crucial role. Following the synthesis of electroactive molecules such as tetrathiafulvalene (TTF) derivatives and their proper (electro)-crystallization, it is well known that the precise solid state organization of these partially oxidized molecules subtly influences their electronic properties (conductivity, magnetism). As a consequence, understanding the different interactions occurring in these solids is of outmost importance to rationalize the observed behaviors and thus to conceive new systems. For example, the weak C–H•••X interactions at work between organic radical molecules and X counter ions at the organic/inorganic interface have been shown to interact dynamically with the electronic conducting system,<sup>3,4</sup> revealing important electrostatic contributions to the charge modulation in the conducting stacks. These correlations have been a powerful incentive to further control the interface with stronger and more directional interactions such as hydrogen<sup>5</sup> or halogen bonding.<sup>6,7</sup> Another much less investigated point is the actual symmetry of the donor molecules themselves. Most of the TTF derivatives used so far (TTF, TMTTF, BEDT-TTF, ...) bear four

identical substituents (Form A in scheme 1), hence a D<sub>2h</sub> symmetry. Another extensively investigated series are the so called dissymmetrical TTFs such as *o*-Me<sub>2</sub>TTF or EDT-TTF (Form B in scheme 1, R<sub>1</sub> ≠ R<sub>2</sub>), with C<sub>2v</sub> symmetry. On the other hand, TTFs with Form C (Scheme 1, R<sub>1</sub> ≠ R<sub>2</sub>) have been much less investigated (Tables S1–S3 in ESI<sup>†</sup>). These compounds, such as BET-TTF or α-DT-TTF, are prepared as a mixture of *Z* and *E* isomers. Successful attempts to separate and crystallize both isomers of such TTFs are scarce,<sup>8,9</sup> since a *Z-E* isomerism process takes place in the presence of traces of acid.<sup>10</sup> Furthermore, upon oxidation to the radical cation, the central C=C bond is weakened, favoring also the *Z-E* isomerism.<sup>11</sup>



**Scheme 1** Tetrathiafulvalene derivatives with different substitution patterns

<sup>a</sup> Institut des Sciences Chimiques de Rennes, Université Rennes 1, UMR CNRS 6226, Campus de Beaulieu 35042 Rennes, France.

<sup>b</sup> Institut de Ciència de Materials de Barcelona (CSIC), Campus de la UAB, E-08193 Bellaterra, Spain.

<sup>c</sup> Laboratoire de Physique des Solides, Université Paris-Sud, UMR CNRS 8502, Bât. 510, 91405 Orsay, France.

<sup>†</sup> Electronic supplementary information (ESI) available: Tables S1–S3 of reported (*Z,E*)-TTF derivatives, Figures S1–S3. For ESI and crystallographic data (CCDC 1428793 and 1428794), see DOI: 10.1039/x0xx00000x

As a consequence, the salts of Form C TTFs are most often found, either as a mixture of *Z* and *E* isomers disordered on one single position (hence an averaged Form A  $D_{2h}$  symmetry),<sup>12,13</sup> or as a pure centrosymmetric *E* isomer known to favor more compact structures (see Tables S1–S3).<sup>14</sup>

We report here a mixed-valence cation radical salt of the Form C iodinated TTF derivative (*Z,E*)- $\text{Me}_2\text{I}_2\text{-TTF}$  (Scheme 1) with the  $\text{Br}^-$  anion, where the two *Z* and *E* isomers of the donor molecule do co-crystallize, but into segregated columns, each of them with a different charge localization pattern and associated electronic structure. The system also demonstrates the important role of the halogen bonding interactions taking place between cation radical and anion to stabilize this highly specific electronic structure.

The neutral donor molecule<sup>9</sup>  $\text{Me}_2\text{I}_2\text{TTF}$  was obtained from the successive lithiation/iodination reaction of the (*Z,E*)- $\text{Me}_2\text{TTF}$  mixture. It crystallizes in the monoclinic system, space group  $P2_1/n$ , with one molecule on an inversion center, hence with the *E*-geometry (Fig. S1 in ESI<sup>†</sup>). Bond distances are collected in Table 1. In the solid, there is no halogen bonding interaction as the shortest  $\text{I}\cdots\text{I}$  contacts exceed 4.32 Å. Its electrocrystallization in the presence of *n*- $\text{Bu}_4\text{NBr}$  in  $\text{CH}_2\text{Cl}_2$  afforded black needles on the anode. The bromide salt crystallizes in the monoclinic system, space group  $P2_1/n$ . Both *Z* and *E* isomers are present (Fig. 1), with one *Z*- $\text{Me}_2\text{I}_2\text{TTF}$ , one bromide anion and one  $\text{CH}_3\text{CN}$  molecule in general position, together with two *E*- $\text{Me}_2\text{I}_2\text{TTF}$  molecules (noted  $E_1$  and  $E_2$ ), each of them on an inversion center. Altogether, it corresponds to a mixed valence state with 2:1 stoichiometry,  $[\text{Z-Me}_2\text{I}_2\text{TTF}][\text{E-Me}_2\text{I}_2\text{TTF}]\text{Br}\cdot\text{CH}_3\text{CN}$ .

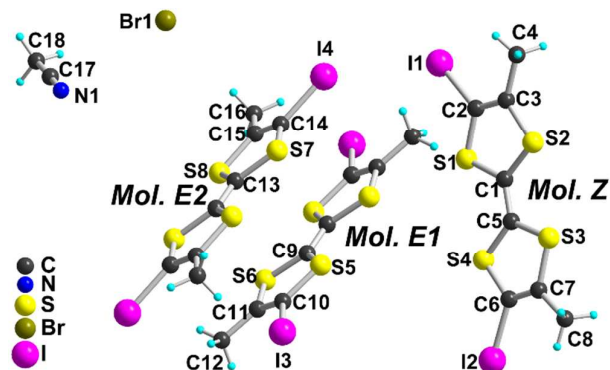
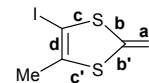


Fig. 1 Detail of the asymmetric unit in the bromide salt

The central C=C as well as the neighboring C–S bond lengths have been shown to be particularly sensitivity to the TTF charge. As shown in Table 1, the recurrent C=C lengthening and associated C–S shortening accompanying the TTF oxidation is well observed here and, more importantly, in a comparable way within the three crystallographically independent molecules. A difference can be found between the two  $E_1$  and  $E_2$  molecules, the formed being apparently slightly more oxidized. Despite this mixed-valence state, the salt behaves as a semiconductor (Fig. S2 in ESI<sup>†</sup>), with a room

temperature conductivity  $\sigma_{\text{RT}} = 0.035 \text{ S cm}^{-1}$  and an activation energy of 0.17 eV (2000 K).

Table 1 Intramolecular bond lengths within the TTF core in  $\text{Me}_2\text{I}_2\text{TTF}$  and its salt.



	<i>E</i>	<i>Z</i> in salt	$E_1$ in salt	$E_2$ in salt
a	1.349(8)	1.380(12)	1.377(12)	1.368(15)
b	1.762(6)	1.738(10), 1.724(9)	1.723(9)	1.753(10)
b'	1.761(6)	1.745(9), 1.745(10)	1.743(10)	1.756(10)
c	1.749(6)	1.727(11), 1.749(10)	1.724(10)	1.758(9)
c'	1.760(6)	1.750(9), 1.765(10)	1.741(11)	1.758(10)
d	1.317(8)	1.331(14), 1.340(14)	1.339(14)	1.343(13)

The salt is also characterized by a segregation of the two *Z* and *E* isomers into separated stacks running along the *a* direction and alternating with each other along the *c* direction into (*ac*) slabs (Fig. 2a). The bromide anions and  $\text{CH}_3\text{CN}$  molecules are interspersed in-between these organic slabs. As shown in Fig. 2b, the bromide anion is interacting strongly with four different iodine atoms of four different molecules while the embedded  $\text{CH}_3\text{CN}$  molecule is not involved in halogen bonding. The corresponding distances and angles are collected in Table 2 and point for a rather short and strong interaction, comparable to those found in other halogen-bonded bromide salts.<sup>6,15</sup> Note also that the  $E_1$  molecule (bearing I3) exhibits a notably shorter (by 0.1 Å) halogen bond to  $\text{Br}^-$  than the  $E_2$  one (bearing I4).

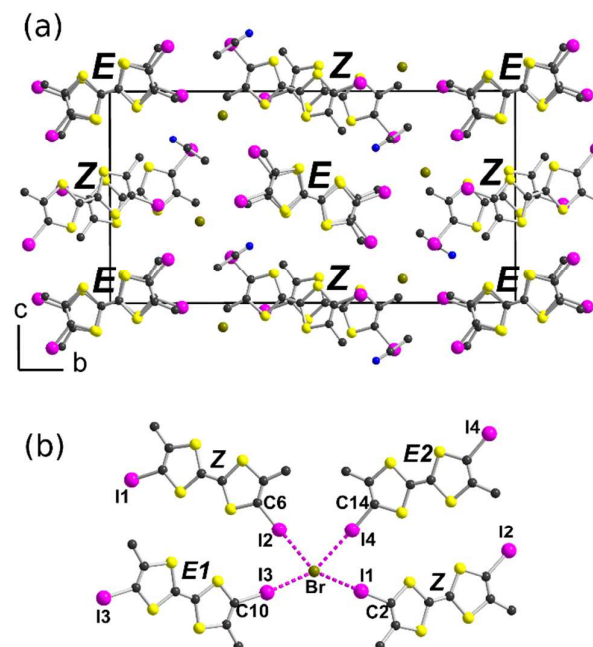
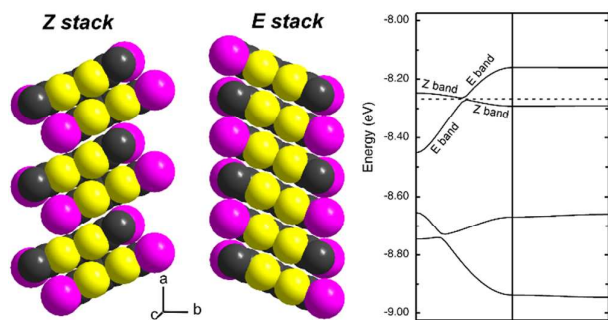


Fig. 2 (a) Projection view of the unit cell of  $[\text{Me}_2\text{I}_2\text{TTF}]\text{Br}\cdot\text{CH}_3\text{CN}$  along the *a* axis. (b) Detail of the halogen bonding interactions.

**Table 2.** Halogen bond characteristics. The reduction ratio RR is defined as the ratio between the I•••Br distance and 3.83 Å, the sum of the I (1.98 Å) and Br (1.85 Å) van der Waals radii.

Halogen	I•••Br (Å)	RR	C–I•••Br (°)
I1	3.246(5)	0.85	176.0(2)
I2	3.300(5)	0.86	178.3(3)
I3	3.245(4)	0.85	173.6(2)
I4	3.348(7)	0.87	175.6(2)

As mentioned above, each partially oxidized slab is composed of segregated stacks of either Z or E molecules. A side view of each of them (Fig. 3) shows that the Z stack is strongly dimerized while the E stack, made of two alternating crystallographically independent  $E_1$  and  $E_2$  molecules, each of them on an inversion center, is uniform by symmetry. These features are confirmed by the calculated  $\beta_{\text{HOMO-HOMO}}$  interaction energies. In the Z stacks, the intra-dimer interaction amounts to  $-0.368$  eV while it reaches only 0.050 eV for the inter-dimer interaction. Within the E stacks, a uniform  $\beta_{\text{HOMO-HOMO}}$  interaction is found at  $-0.306$  eV.



**Fig. 3** Detail of the Z and E stacks (left), and the calculated band structure (right). The dotted line refers to the  $\frac{3}{4}$ -filling of the system and  $\Gamma = (0, 0)$ ,  $X = (a^*/2, 0)$  and  $Z = (c^*/2, 0)$ .

Altogether, this interaction network gives rise to the calculated extended Hückel band structure shown in Fig. 3. Four bands are obtained as a superposition of the essentially independent Z and E stacks (Fig. S3 in ESI†). A sizeable band dispersion along the chains direction ( $\Gamma$ –X) is observed only for the regular Z stack while the E bands are only weakly dispersive. A very small forbidden band crossing is calculated between the two upper bands. Inter-stack interactions (see  $\Gamma$ –Z) are negligible. This description however contradicts the observed semi-conducting behavior with large activation energy. It clearly indicates that strong electronic repulsions have to be taken into account and that such a band description with paired electrons is not pertinent here. In other words, electronic repulsions are strong enough and charge localization takes place on the two chains, with however striking differences between them. Indeed, in such systems where long range electronic repulsions dominate, a so-called Wigner lattice of localized charges can be stabilized, leading to a semi-conducting behavior.<sup>2</sup> The system can adopt essentially two different electronic structures, either a charge localization on the molecular sites (described as Charge Order or CO) or a

charge localization between two molecules within dyads, described as Bond Order Wave (BOW) or dimer-Mott (DM), as illustrated in Fig. 4.<sup>16,17</sup>

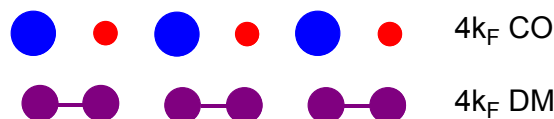


**Fig. 4** Schematic representation of the electronic description of the  $4k_F$  Charge-Order and Dimer-Mott states in quarter-filled systems. The violet color corresponds to the uniform  $\frac{1}{2}$  charge while the red and blue ones to  $\frac{1}{2} + \delta$  and  $\frac{1}{2} - \delta$ .

In the CO state, molecules bear alternatively an excess and a depletion of charge  $\delta$  ( $0 < \delta \leq \frac{1}{2}$ ), that is  $(\frac{1}{2} + \delta, \frac{1}{2} - \delta)$ , while in the DM state, the molecules dimerize but keep the average  $+\frac{1}{2}$  charge. A DM ground state is found for example in the quarter filled MEM(TCNQ)<sub>2</sub> salt below 335 K,<sup>18</sup> while the CO state has been identified for example in the whole (TMTTF)<sub>2</sub>X series where the  $T_{\text{CO}}$  varies from 230 and 65 K depending on the counter ion X.<sup>2c</sup> On the other hand, coexistence of both CO and DM states within the very same system has been only evidenced in the low temperature phases of some very specific salts with tetragonal symmetry, such as (DI-DCNQI)<sub>2</sub>Ag (space group I4<sub>1</sub>/a)<sup>19,20</sup> or (o-Me<sub>2</sub>TTF)<sub>2</sub>X (X = Cl, Br; space group  $\bar{1}42d$ ),<sup>21</sup> but without structural confirmation in the latter.

The salt reported here combines efficiently these two  $4k_F$  states at room temperature. The Z chains adopt indeed the dimer-Mott (DM) structure with a strong dimerization and a fixed  $\frac{1}{2}$  charge on each Z molecule. On the other hand, in the uniform ( $E_1E_2$ ) chains, we have noted above that the  $E_1$  molecule was slightly more oxidized than the  $E_2$  one. It indicates that these E chains adopt a CO state, providing one rare example of a pure CO chain where there is only charge disproportionation on the two crystallographically independent  $E_1$  and  $E_2$  molecules, without dimerization since intra-stack interactions are uniform. This CO state is further confirmed by the specific details of the cation-anion interaction mediated here by the halogen bonding (Fig. 2b). Indeed, we have noted that the bromide anion is closer to the more oxidized  $E_1$  molecule than to  $E_2$ . Such effects have been recently well established in other CO systems such as (TMTTF)<sub>2</sub>X,<sup>3</sup>  $\alpha$ -(BEDT-TTF)<sub>2</sub>I<sub>3</sub>,<sup>4</sup> or  $\delta$ -(EDT-TTF-CONMe<sub>2</sub>)<sub>2</sub>Br,<sup>22</sup> where the anion is "linked" to the radical cations, but through weak C–H hydrogen bonds. In these salts, below the metal-insulator transition at  $T_{\text{CO}}$ , a shift of the anion toward the most oxidized molecule is indeed observed. We demonstrate here for the first time that such effects can be also efficiently transmitted through halogen bonding rather than C–H•••X hydrogen bonding interactions.

In conclusion, we have identified a halogen bonded, mixed valence, conducting salt where two different types of charge ordering patterns, namely Charge Order (CO) and Dimer-Mott (DM) coexist at room temperature, thanks to the remarkable co-crystallization and segregation of Z and E isomers of the iodinated Me<sub>2</sub>I<sub>2</sub>TTF donor molecule. The halogen bonding

interaction to the counter ion is shown here to correlate with the state of charge of the donor molecule, a further demonstration of charge-assisted halogen bonding.<sup>23,24</sup>

This work was supported by MINECO (Spain) through Grant FIS2012-37549-C05-05, Generalitat de Catalunya (2014 SGR301), and ANR (France) through Grant 08-BLAN-0091.

## Notes and references

‡ Crystal data for Me<sub>2</sub>I<sub>2</sub>TTF: C<sub>8</sub>H<sub>6</sub>I<sub>2</sub>S<sub>4</sub>, *M* = 484.17, monoclinic, space group P2<sub>1</sub>/n, *T* = 150(2) K, *a* = 6.2612(3), *b* = 15.4368(8), *c* = 6.6118(4) Å, β = 96.285(2)°, *V* = 635.21(6) Å<sup>3</sup>, *Z* = 2, ρ<sub>calcd</sub> = 2.532 g cm<sup>-3</sup>, *R*<sub>1</sub>(*wR*<sub>2</sub>) = 0.0365 (0.0919) and *S* = 1.203 for 1459 reflections and 1404 reflections with *I* > 2σ(*I*). The iodine atom and the methyl group are slightly disordered, with a 96.5/3.5 distribution. CCDC 1428793.

§ Crystal data for [Me<sub>2</sub>I<sub>2</sub>TTF]Br•CH<sub>3</sub>CN: C<sub>18</sub>H<sub>15</sub>BrI<sub>4</sub>NS<sub>8</sub>, *M* = 1089.30, monoclinic, space group P2<sub>1</sub>/n, *T* = 150(2) K, *a* = 27.120(7), *b* = 27.120(7), *c* = 14.215(4) Å, β = 95.259(10)°, *V* = 3028.1(13) Å<sup>3</sup>, *Z* = 4, ρ<sub>calcd</sub> = 2.389 g cm<sup>-3</sup>, *R*<sub>1</sub>(*wR*<sub>2</sub>) = 0.0536 (0.1420) and *S* = 1.061 for 6908 reflections and 4628 reflections with *I* > 2σ(*I*). CCDC 1428794.

- P. Batail, *Chem. Rev.*, 2004, **104**, 4887–4890.
- (a) J.-P. Pouget, *Physica B*, 2012, **407**, 1762–1770; (b) H. Seo, C. Hotta and H. Fukuyama, *Chem. Rev.*, 2004, **104**, 5005–5036; (c) D. Jérôme, *Chem. Rev.*, 2004, **104**, 5565–5592.
- K. Medjanik, A. Chernenkaya, S. A. Nepijko, G. Öhrwall, P. Foury-Leylekian, P. Alemany, E. Canadell, G. Schönhense and J.-P. Pouget, *Phys. Chem. Chem. Phys.*, 2015, **17**, 19202–19214.
- P. Alemany, J.-P. Pouget and E. Canadell, *Phys. Rev. B*, 2012, **85**, 195118 (1–10)
- M. Fourmigué and P. Batail, *Chem. Rev.*, 2004, **104**, 5379–5418
- (a) T. Imakubo, H. Sawa and R. Kato, *Synth. Metals*, 1995, **73**, 117; (b) M. Fourmigué, *Struct. Bond.*, 2008, 126, 181–207; (c) M. Fourmigué and J. Liefbrig, *Top. Curr. Chem.* 2015, **359**, 91–113 (d) M. Fourmigué, *Curr. Op. Solid State Mater. Sc.* **2009**, **13**, 36–45.
- (a) T. Imakubo, T. Shirahata, K. Hervé and L. Ouahab, *J. Mater. Chem.*, 2006, **16**, 162–173; (b) J. Liefbrig, R. Le Pennec, O. Jeannin, P. Auban-Senzier and M. Fourmigué, *CrystEngComm*, 2013, **15**, 4408–4412; (c) K.-S. Shin, O. Jeannin, M. Brezgunova, S. Dahaoui, E. Aubert, E. Espinosa, P. Auban-Senzier, R. Świetlik, A. Frackowiak and M. Fourmigué, *Dalton Trans.*, 2014, **43**, 5280–5291.
- (a) C. Rovira, J. Veciana, N. Santalo, J. Tarres, J. Cirujeda, E. Molins, J. Llorca and E. Espinosa, *J. Org. Chem.*, 1994, **59**, 3307–3313; (b) R. A. L. Silva, A. I. Neves, M. L. Afonso, I. C. Santos, E. B. Lopes, F. Del Pozo, R. Pfattner, M. Mas-Torrent, C. Rovira, M. Almeida and D. Belo, *Eur. J. Inorg. Chem.*, 2013, 2440–2446; (c) O. Jeannin and M. Fourmigué, *Chem.-Eur. J.*, 2006, **12**, 2994–3005.
- R. Makhoul, Y. Kumamoto, A. Miyazaki, F. Justaud, F. Gendron, J.-F. Halet, J.-R. Hamon and C. Lapinte, *Eur. J. Inorg. Chem.*, 2014, 3899–3911.
- (a) A. Souizi, A. Robert, P. Batail and L. Ouahab, *J. Org. Chem.* 1987, **52**, 1610–1611; (b) M. Giffard, P. Frère, A. Gorgues, A. Riou, J. Roncali and L. Toupet, *J. Chem. Soc., Chem. Commun.* 1993, 944–945.
- E. Fanghänel, L. van Hinh, G. Schukat and J. Patzsch, *J. Prakt. Chem.*, 1989, **331**, 479–485
- (a) S. S. Khasanov, A. Perez-Benitez, B. Zh. Narymbetov, L. V. Zorina, R. P. Shibaeva, J. Singleton, A.-K. Klehe, V. N. Laukhin, J. Vidal-Gancedo, J. Veciana, E. Canadell and C. Rovira, *J. Mater. Chem.*, 2002, **12**, 432–441; (b) J. Tarres, N. Santalo, M. Mas, E. Molins, J. Veciana, C. Rovira, S. Yang, H. Lee, D. O. Cowan, M.-L. Doublet and E. Canadell, *Chem. Mater.*, 1995, **7**, 1558–1567.
- R. A. L. Silva, A. I. S. Neves, E. B. Lopes, I. C. Santos, J. T. Coutinho, L. C. J. Pereira, C. Rovira, M. Almeida and D. Belo, *Inorg. Chem.*, 2013, **52**, 5300–5306.
- (a) A. Ranganathan, A. El-Ghayoury, C. Mézières, E. Harté, R. Clérac and P. Batail, *Chem. Commun.*, 2006, 2878–2880; (b) J. Tarres, M. Mas, E. Molins, J. Veciana, C. Rovira, J. Morgado, R. T. Henriques and M. Almeida, *J. Mater. Chem.*, 1995, **5**, 1653–1658; (c) T. Higashino, Y. Akiyama, H. Kojima, T. Kawamoto and T. Mori, *Crystals*, 2012, **2**, 1222–1238.
- (a) H. Bock and S. Holl, *Z. Naturforsch. B*, 2001, **56**, 152; (b) S. Triguero, R. Llusar, V. Polo and M. Fourmigué, *Cryst. Growth Des.*, 2008, **8**, 2241; (c) P. Metrangolo, F. Meyer, T.; Pilati, G. Resnati and G. Terraneo, *Chem. Commun.*, 2008, 1635–1637; (d) J. Liefbrig, O. Jeannin and M. Fourmigué, *J. Am. Chem. Soc.*, 2013, **135**, 6200–6210
- J.-P. Pouget, *Physica B*, 2015, 460, 45–52.
- J.-P. Pouget, P. Foury-Leylekian, P. Alemany and E. Canadell, *Phys. Status Solidi B*, 2012, **249**, 937–942
- S. Huizinga, J. Kommandeur, G. A. Sawatzky, B. T. Thole, K. Kopinga, W. J. M. de Jonge, and J. Roos, *Phys. Rev. B*, 1979, **19**, 4723–4732.
- (a) R. Kato, H. Kobayashi and A. Kobayashi, *J. Am. Chem. Soc.*, 1989, **111**, 5224–5232; (b) T. Itou, K. Kanoda, K. Murata, T. Matsumoto, K. Hiraki, and T. Takahashi, *Phys. Rev. Lett.*, 2004, **93**, 216408; (c) T. Itou, K. Kanoda, K. Hiraki, T. Takahashi, K. Murata, and T. Matsumoto, *Phys. Rev. B*, 2005, **72**, 113109.
- T. Kakiuchi, Y. Wakabayashi, H. Sawa, T. Itou, and K. Kanoda, *Phys. Rev. Lett.*, 2007, **98**, 066402.
- (a) P. Foury-Leylekian, P. Auban-Senzier, C. Coulon, O. Jeannin, M. Fourmigué, C. Pasquier and J.-P. Pouget, *Phys. Rev. B*, 2011, **84**, 195134; (b) R. Abderraba, R. Laversanne, E. Dupart, C. Coulon, P. Delhaes, and C. Hauw, *J. Phys. Colloq. C3*, 1983, **44**, C3-1243; (c) M. Fourmigué, E. W. Reinheimer, K. R. Dunbar, P. Auban-Senzier, C. Pasquier and C. Coulon, *Dalton Trans.*, 2008, 4652–4658.
- L. Zorina, S. Simonov, C. Mézière, E. Canadell, S. Suh, S. E. Brown, P. Foury-Leylekian, P. Fertey, J.-P. Pouget and P. Batail, *J. Mater. Chem.*, 2009, **19**, 6980–6994; (b) P. Auban-Senzier, C. Pasquier, D. Jérôme, S. Suh, S. E. Brown, C. Mézière, and P. Batail, *Phys. Rev. Lett.*, 2009, **102**, 257001/1–257001/4.
- (a) J. Liefbrig, O. Jeannin, A. Frackowiak, I. Olejniczak, R. Świetlik, S. Dahaoui, E. Aubert, E. Espinosa, P. Auban-Senzier and M. Fourmigué, *Chem. Eur. J.*, 2013, **19**, 14804–14813; (b) O. Makhotkina, J. Liefbrig, O. Jeannin, M. Fourmigué, E. Aubert and E. Espinosa, *Cryst. Growth Des.*, 2015, **15**, 3464–3473.
- (a) F. Zapata, A. Caballero, N. G. White, T. D. W. Claridge, P. J. Costa, V. Félix and P. D. Beer, *J. Am. Chem. Soc.*, 2012, **134**, 11533–11541; (b) S. M. Walter, F. Kniep, L. Rout, F. P. Schmidtchen, E. Herdtweck, and S. M. Huber, *J. Am. Chem. Soc.*, 2012, **134**, 8507–8512; (c) S. Groni, T. Maby-Raud, C. Fave, M. Branca and B. Schöllhorn, *Chem. Commun.*, 2014, 14616–14619; (d) D. Fox, P. Metrangolo, D. Pasini, T. Pilati, G. Resnati and G. Terraneo, *CrystEngComm*, 2008, **10**, 1132–1136.